Bioorganic & Medicinal Chemistry xxx (2015) xxx–xxx

Contents lists available at ScienceDirect

Bioorganic & Medicinal Chemistry

journal homepage: www.elsevier.com/locate/bmc

Design, synthesis and evaluation of XZH-5 analogues as STAT3 inhibitors

Philias Daka [a], Aiguo Liu [b], Chamini Karunaratne [a], Erika Csatary [a], Cameron Williams [a], Hui Xiao [c,d], Jiayuh Lin [c,d], Zhenghu Xu [e], Richard C. Page [a,*], Hong Wang [a,*]

[a] Department of Chemistry and Biochemistry, Miami University, Oxford, OH 45056, USA
[b] Department of Pediatrics, Tongji Medical College, Huazhong University of Science and Technology, Wuhan, Hubei Province 430030, PR China
[c] Center for Childhood Cancer and Blood Diseases, The Research Institute at Nationwide Children's Hospital, Department of Pediatrics, The Ohio State University, Columbus, OH, USA
[d] Molecular, Cellular and Developmental Biology Program, The Ohio State University, Columbus, OH, USA
[e] School of Chemistry and Chemical Engineering, Shandong University, Jinan, PR China

ARTICLE INFO

Article history:
Received 6 September 2014
Revised 3 January 2015
Accepted 15 January 2015
Available online xxxx

Keywords:
STAT3
Inhibitor
SARs
SH2
Small organic molecule
Molecular docking

ABSTRACT

Inhibition of the signaling pathways of signal transducer and activator of transcription 3 (STAT 3) has shown to be a promising strategy to combat cancer. In this paper we report the design, synthesis and evaluation of a novel class of small molecule inhibitors, that is, XZH-5 and its analogues, as promising leads for further development of STAT3 inhibitors. Preliminary SARs was established for XZH-5 and its derivatives; and the binding modes were predicted by molecular docking. Lead compounds with IC_{50} as low as 6.5 μM in breast cancer cell lines and 7.6 μM in pancreatic cancer cell lines were identified.

1. Introduction

Signal Transducer and Activator of Transcription 3 (STAT3) is a transcription factor belonging to a family of seven proteins (STATs) that regulate important cellular processes such as cell survival, immune response, angiogenesis and cell proliferation.[1–3] STAT3 is activated by phosphorylation on two conserved residues, tyrosine (Tyr_{705}) and serine (Ser_{727}) in response to extracellular signaling molecules such as cytokines and growth factors.[4,5] Once phosphorylated, a $pTyr_{705}$ residue from a STAT3 protomer binds in trans to the Src homology 2 (SH2) domain of another STAT3 protomer to facilitate formation of the STAT3 dimer. The dimeric form translocates into the nucleus where it binds to DNA at specific promoter regions and induces transcription of targeted genes.[6,7] For normal functioning of the cell under physiological conditions, this process is highly regulated. However, overexpression and constitutive high levels of STAT3 are frequently detected within tumors from prostate, breast, head and neck cancer patients with advanced disease and in other human cancer cell lines.[8,9] Growing evidence shows that the overexpression and persistent activation of STAT3 promotes tumorigenesis directly by stimulating cell proliferation and inhibiting apoptosis in human cancer cells.[10] Due to the role of STAT3 in promoting human malignancies, its inhibition is an attractive target to combat cancer.[11–13]

Several classes of compounds have been developed that use either direct or indirect mechanisms to inhibit STAT3. Indirect inhibition involves targeting janus kinase (JAK), or introducing antisense oligonucleotides, siRNAs, dominant-negative mutant, decoy oligonucleotides, or G-quartet oligonucleotides that regulate upstream activation leading to phosphorylation.[14–19] Specifically, small molecules like pyridone-6,[20] and natural product based indirubin,[21] resveratrol,[22] cucurbitacin analogues,[23,24] and capsaicin[25] have been explored in this area. Unfortunately, most of these small molecule candidates are unsuitable therapeutics due to off-target pathway effects resulting in undesirable side effects. Under the direct strategy, inhibition of STAT3 dimerization has been the major focus as it constitutes the crucial step in STAT3 activation. Here, both peptidomimetic[26–33] and nonpeptidomimetic[34,35] drugs have been examined. In vitro studies have demonstrated that peptide-based inhibitors bind strongly to STAT3 resulting in high affinities; however, these peptide-based inhibitors usually suffer from low cellular permeability and rapid clearance from the blood

* Corresponding authors. Tel.: +1 513 529 2824, +1 513 529 2281.
E-mail addresses: pagerc@miamioh.edu (R.C. Page), wangh3@miamioh.edu (H. Wang).

http://dx.doi.org/10.1016/j.bmc.2015.01.025
0968-0896/

stream. In contrast, while non peptide-based inhibitors can be designed to exhibit excellent cellular permeability and extended bioavailability, current nonpeptidomimetic inhibitors display low binding affinity. Perhaps the most striking point is that despite tremendous effort that has been channeled in the design of STAT3 inhibitors, no inhibitors have progressed to clinical trials.[31] It is imperative that new small-molecule candidates be identified and optimized to inhibit STAT3. Here we report the preliminary Structure Activity Relationships (SARs) of XZH-5 (**1a**) and its derivatives (Fig. 1), a novel candidate molecule previously reported to inhibit STAT3 phosphorylation and elicit apoptosis in human hepatocellular carcinoma cell.[36–38]

2. Results and discussion

2.1. The design and synthesis of inhibitors

XZH-5 is a recently identified small molecule inhibitor binding to STAT3 SH2 domain.[36–38] XZH-5 has shown inhibitory activity toward STAT3 phosphorylation in human hepatocellular carcinoma cells,[36] rhabdomyosarcoma cells,[37] breast and pancreatic cancer cells .[38] XZH-5 and its derivatives presented here represent novel class of organic molecules. XZH-5 and its analogues were designed to bind the phosphotyrosine 705 (pY705) binding pocket and the neighboring hydrophobic side-pocket. A carboxylate moiety derived from an amino acid, that is, L-histidine, mimics phosphate of pTyr (Fig. 1A), while trifluoromethyl-benzene is used to initiate hydrophobic interaction with the side pocket. The combination of urea and peptidyl linkers provides appropriate distances between the two binding sites. The urea and peptidyl linkers are expected to capture H-bonds since the space between the two sites is rich in H-bond acceptors and donors. The urea linker also serves to reduce the peptidomic character of the inhibitors.

A large number of structural variations can be derived from XZH-5 due to its structural flexibility. Figure 1B illustrates the modifiable groups of XZH-5 and its derivatives (R^1–R^4). The goal of this work, however, is to establish preliminary SARs and gain fundamental knowledge about the relative importance of each modifiable group of this novel class of inhibitors.

The synthesis of XZH-5 (**1a**) and its analogues (**1b**–**1n**) follow a general route starting from amino acid histidine (Scheme 1). Regioselective alkylation of histidine was carried out according to a procedure slightly modified from Cohen et al. protocol[39] to generate the alkyl 2-amino(1-alkyl-1*H*-imidazol-4-yl) propanoate (**A**). Esterification of the free carboxylic acid group was performed before the cyclization step and after the alkylation step using $SOCl_2$ and R^1OH. *N*-Alkyl histidine alkyl ester (**A**) was then coupled to the appropriate *N*-Boc protected amino acid to generate **B**. It should be noted that, depending on the amino acids that were in play, different coupling reagents were used in order to obtain efficient coupling. Deprotection of the Boc group of **B** followed by coupling with 1-isocyanato-3,5-bis(trifluoromethyl) benzene gave the desired product **1** (Scheme 1). Using Scheme 1, fourteen inhibitors were prepared (Fig. 2).

2.2. Modifications of trifluoromethyl and histidine moieties (R^2 and fluorinated aryl group)

XZH-5 (**1a**) provides a modifiable scaffold with measurable and significant inhibitory activity against human pancreatic (PANC-1, HPAC and SW1990) and breast (MDA-MB-231) cancer cell lines. In the absence of structural data for the human STAT3 SH2 domain we focused initial synthetic efforts on the trifluoromethyl and histidine moieties of XZH-5 (**1a**). We synthesized **1n** (Fig. 2) carrying only one trifluoromethyl group and tested the compound against a suite of pancreatic and breast cancer cell lines. The IC_{50} for **1n** was 61.9 μM against the PANC-1 cell line (Table 1) while no detectable inhibition was observed against either HPAC or SW1990 pancreatic cancer cell lines or an MDA-MB-231 breast cancer cell line. The significant declines in inhibitory activity suggest that both trifluoromethyl groups are required, presumably due to modulation of lipophilicity, pK_a or electrostatics of the bifunctionalized phenyl ring.[40]

Turning our focus to the histidine moiety we synthesized variants (Fig. 2), which removed the imidazole R^2 substituent (**1m**). **1m** exhibited poor inhibitory activity compared to **1a**, suggesting that the imidazole ring is a crucial component and that it should be τ-substituted. Furthermore, the incorporation a longer alkyl substitute, that is, ethyl group at the τ-position of the imidazole ring, enhanced the inhibitory activity by roughly two fold in all four cancer cell lines (compare **1a** and **1k** in Table 1). In comparison to the histidine side chain, hydrolysis of the histidinyl ester groups from **1a** and **1b** to free carboxylic acids, generating **1e** and **1f**, were similarly deleterious resulting in IC_{50} values greater than 100 μM (Table 1). The rationale for the negative effect upon binding due to the free carboxylic acids from **1e** and **1f** is unclear, although a decrease in lipophilicity or the introduction of unfavorable electrostatics may be at play.

2.3. Modification of the central valine moiety (R^3)

Turning our attention to the central valine moiety of XZH-5 (**1a**) we synthesized 8 inhibitors utilizing different amino acids to produce inhibitors with varying R^3 groups (Scheme 1). The observed inhibitory activity of compounds **1c**, **1d** and **1g**–**1j** identifies a range of R^3 groups with optimal steric size. For example, when R^3 is a methyl group (**1b**) the IC_{50} increases to 50–100 μM against the PANC-1 cell line and undetectable inhibition against HPAC, SW1990 and MDA-MB-231 cell lines. In comparison, the bulkier R^3 groups from **1c**, **1d**, and **1l** result in IC_{50} values near 10 μM across all tested cell lines. While an aromatic phenyl group as R^3 (**1g**) also showed much increased inhibitory activity, further expanding the aromatic moiety with an indole ring resulted in reduced inhibitory effect of **1h** in PANC-1 cells by two folds (compare **1g** and **1h** in Table 1).

To understand the role of R^1–R^4 we conducted in silico docking studies for **1a**–**1n** against the STAT3 SH2 domain. Table 2 shows the docking data of these compounds. Here we have utilized a human STAT3 SH2 domain homology model, rebuilt with Rosetta side chain repacking, paired with a robust molecular modeling

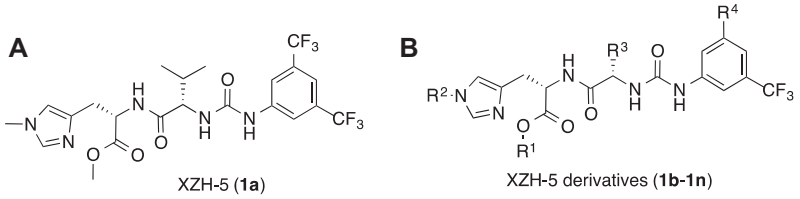

Figure 1. (A) Structure of the STAT3 inhibitor XZH-5 (**1a**). (B) XZH-5 derivatives with modifiable groups.

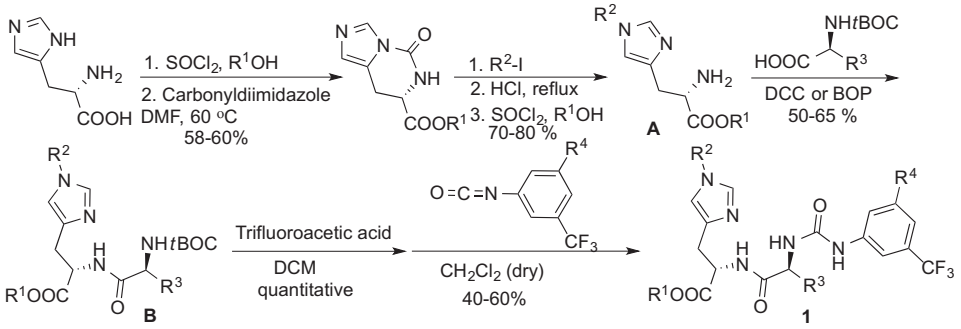

Scheme 1. Synthesis of XZH-5 analogues.

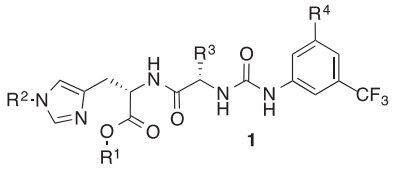

	R^1	R^2	R^3	R^4
1a	Me	Me	$CH(CH_3)_2$	CF_3
1b	Me	Me	Me	CF_3
1c	Me	Me	$CH_2CH(CH_3)_2$	CF_3
1d	Me	Me		CF_3
1e	OH	Me	$CH(CH_3)_2$	CF_3
1f	OH	Me	Me	CF_3
1g	Me	Me	Bn	CF_3
1h	Me	Me	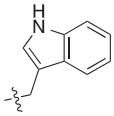	CF_3
1i	Me	Me	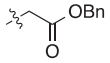	CF_3
1j	Me	Me	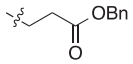	CF_3
1k	Me	Et	$CH(CH_3)_2$	CF_3
1l	Me	Me	$C(CH_3)_3$	CF_3
1m	Me	H	$CH(CH_3)_2$	CF_3
1n	Me	Me	$CH(CH_3)_2$	H

Figure 2. Structure of inhibitors.

protocol allowing for full flexibility of XZH-5 analogues and the STAT3 SH2 domain. Rosetta repacking of proteins prior to docking has been shown to improve the reliability of docking results.[41–43] Enabling full flexibility of XZH-5 and the protein incorporates physically realistic representations of the molecules in solution.[42]

Throughout docked models for **1c**, **1d**, **1g**, **1k**, and **1l** two key interactions are observed. First, the CF_3-substituted phenyl ring packs in a nearly identical manner against the side chains of Lys_{626} and Gln_{633}. Second, the R^1 and R^3 groups participate in hydrophobic packing that buttresses the inhibitor in a position straddling the $pTyr_{705}$ binding site with R^3 and R^1 bound in SH2 domain pockets 1 and 2 (Fig. 3), respectively. Inhibitors **1c**, **1d**, and **1k** all feature nearly identical backbone positions, likely due

Table 1
IC_{50} (μM) on different cell lines

Inhibitor	PANC-1	HPAC	MDA-MB-231	SW1990
1a	24.7	17.4	15.5	17.9
1b	50–100	ND	ND	ND
1c	16.8	13.2	10.6	9.1
1d	10.1	7.6	6.5	8.3
1e	>100	ND	ND	ND
1f	>100	ND	ND	ND
1g	16.1	9.6	6.8	10.8
1h	31.4	ND	ND	ND
1i	68.6	ND	ND	ND
1j	85.5	ND	ND	ND
1k	11.1	9.5	7.6	9.4
1l	8.8	9.8	9.4	8.5
1m	98.4	ND	ND	ND
1n	61.9	ND	ND	ND

Note: ND = not determined.

to similar interactions between tertiary carbon centers at the β-carbon (**1d** and **1k**) or γ-carbon (**1c**) of R^3 that allows the lone hydrogen of the tertiary carbon center to pack against a cleft formed by Ile_{634} and Gln635. In contrast, relative to **1c**, **1d**, and **1k**, the backbone and methyl ester positions in **1l** are perturbed due to a quaternary carbon center at the β-position of R^3. Although the additional methyl group at the β-position increases the steric size, the *t*-butyl group remains bound in pocket 1. In comparison, while the histidinyl methylester from **1c** is rotated with respect to the positions in **1d**, **1g** and **1k**, the backbone, trifluoromethyl and τ-substituted histidine sidechain occupy nearly identical positions. Despite minor alterations in backbone position, as mediated by the presence of a tertiary or quaternary carbon center in R^3, each inhibitor (**1d**, **1k** and **1l**) makes similar electrostatic contacts with STAT3.

3. Conclusion

We designed and synthesized a novel class of organic compounds derived from XZH-5 (**1a**) as inhibitors targeting STAT3 SH2 domain. Our synthetic scheme allows **1a** to serve as a versatile scaffold for identification of improved STAT3 inhibitors. We paired in silico docking with inhibitory studies against a panel of pancreatic and breast cancer cell lines and identified a set of five improved XZH-5 analogues. The improved STAT3 inhibitors exhibit IC_{50} values near or below 10 μM in PANC-1, HPAC and SW1990 pancreatic cancer cell lines and an MDA-MB-231 breast cancer cell line. Our results identify a discrete range of steric sizes for R^3 as a critical characteristic for optimizing inhibition. Using **1c**, **1d**, **1g**, **1k** and **1l** as a base, our future SAR studies will optimize binding of the τ-substituted histidine group to pocket 2 and explore restrictions and requirements for modification of the histidinyl methylester.

Table 2
Docking data of compounds **1a–1n**

Name	Structure	*c*log*P*[a]	Hydrogen bond acceptors/donors	RosettaDock score[b]	Average IC_{50}[c] (μM)
Scaffold	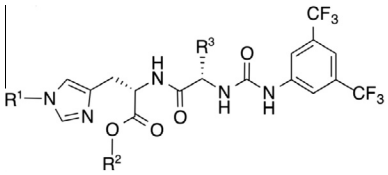	–	–	–	–
1a	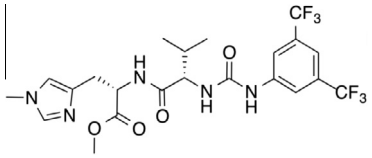	3.44	4/3	−46.3 ± 2.8	18.9
1b	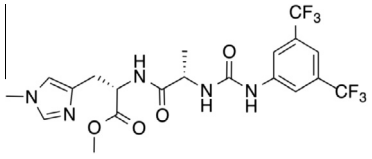	2.48	4/3	NC	>50–100
1c	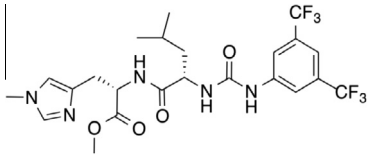	3.80	4/3	−50.8 ± 1.2	12.4
1d	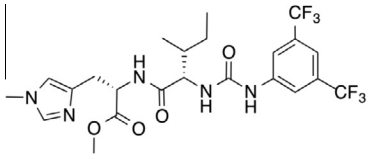	3.80	4/3	−49.4 ± 1.2	8.1
1e	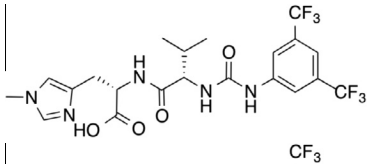	3.12	5/4	−42.8 ± 8.2	>100
1f	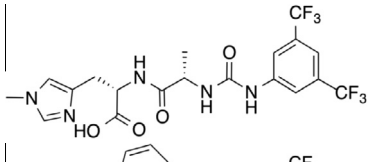	2.15	5/4	NC	>100
1g	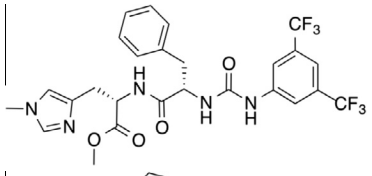	4.07	4/3	−48.8 ± 2.3	10.8
1h	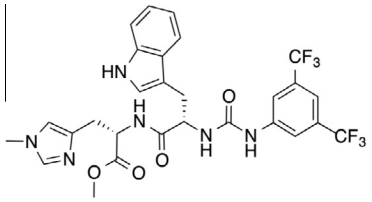	4.20	4/3	−45.5 ± 2.0	>31.4
1i	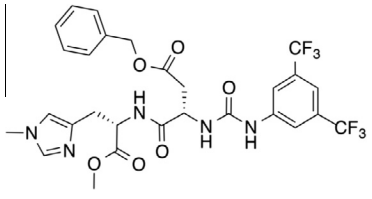	3.43	5/3	−42.2 ± 2.0	>68.6

Table 2 (*continued*)

Name	Structure	clog*P*[a]	Hydrogen bond acceptors/donors	RosettaDock score[b]	Average IC_{50}[c] (μM)
1j	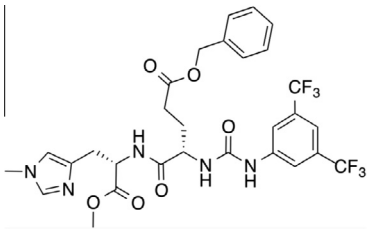	3.79	5/3	−42.3 ± 2.6	>85.5
1k	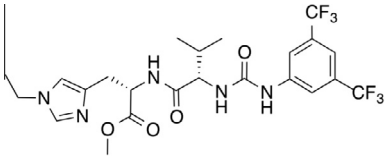	3.75	4/3	−47.6 ± 2.0	9.4
1l	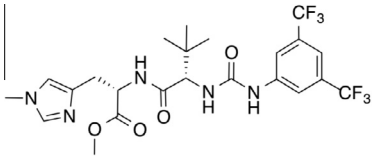	3.84	4/3	−48.0 ± 0.7	9.1
1m	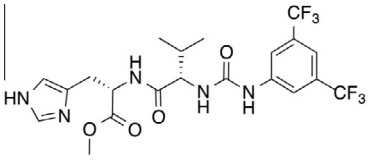	2.56	4/3	−40.5 ± 3.2	>61.9
1n	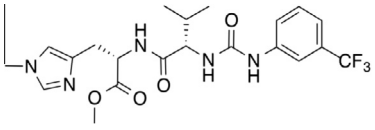	3.49	4/3	−40.8 ±5.9	>29.6

[a] Calculated with XLOGP3.[44] Computation of octanol-water partition coefficients by guiding an additive model with knowledge.
[b] Scores reported as the average of score ± one standard deviation for five low energy structures. NC denotes a docking run that did not converge on a common low-energy docking pose.
[c] >Symbol used for compounds with one or more IC_{50} values above the detection range for inhibition assays against PANC-1, HPAC, MDA-MB-231 or SW1990 cell lines.

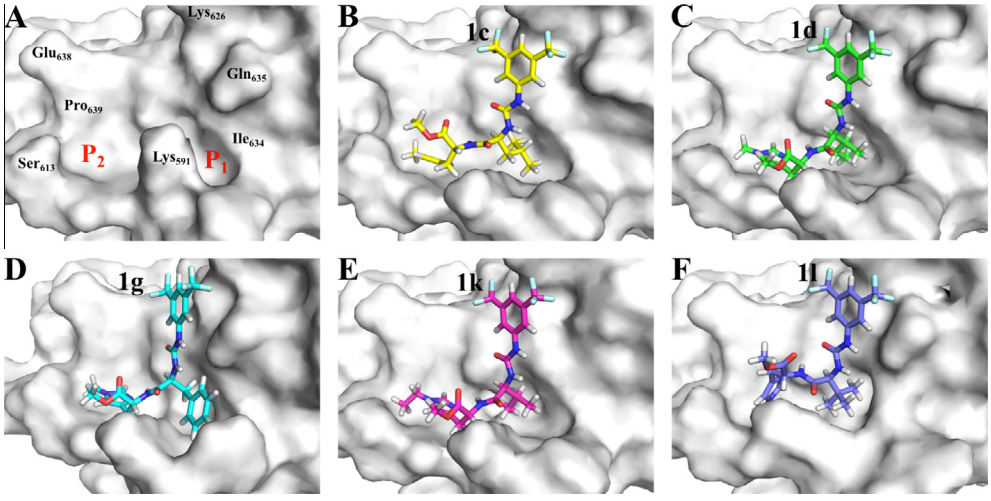

Figure 3. (A) Rosetta-repacked homology model of human STAT3 SH2 domain (grey surface) with binding pockets 1 (P_1) and 2 (P_2) highlighted. (B) Model of **1c** (yellow) bound to human STAT3 SH2 (grey surface). (C) Model of **1d** (green) bound to human STAT3 SH2 (grey surface). (D) Model of **1g** (cyan) bound to human STAT3 SH2 (grey surface). (E) Model of **1k** (magenta) bound to human STAT3 SH2 (grey surface). (F) Model of **1l** (blue) bound to human STAT3 SH2 (grey surface).

4. Experimental

4.1. Biological methods

4.1.1. Molecular modeling

A homology model of human STAT3 SH2 domain was prepared by iTASSER[45] using the mouse STAT3 structure[46] as a template. The human STAT3 homology model was prepacked with Rosetta[47] to generate the starting model for docking with **1c**, **1d**, **1g**, **1k** or **1l**. Initial geometries for XZH-5 analogues **1c**, **1d**, **1g**, **1k** or **1l** were optimized using PHENIX eLBOW[48] for input into OMEGA. Rosetta ligand parameter files were prepared from the final geometries and charges for a family of 256 distinct conformers for each XZH-5 analogue generated using OMEGA.[49] RosettaLigand[42,43] docking calculations allowed for backbone and side-chain flexibility with extra Chi1 and aromatic-Chi2 rotamers for STAT3 SH2 domain with permitted ligand translations away from the starting pose of up to ±5 Å along the *x*, *y* and *z* axes. An ensemble of 20,000 decoys was generated and the top 50 were clustered based upon overall Rosetta energy score (total_score). Representative models were selected from the low energy ensemble.

4.1.2. Cell culture

Procedure is similar to published methods.[38]

4.1.3. Inhibition assays in human cancer cell lines

Cells were seeded in 96-well plates (3000 cells/well) in triplicate, treated with desired concentrations of XZH-5 and its analogues (from **1a** to **1n**) for 72 h. 25 μl of 3-(4,5-dimethylthiazolyl)-2,5-diphenyltetrazolium bromide (MTT, Sigma) was added to each sample and incubated for 3.5 h. Then 100 μl of *N*,*N*-dimethylformamide solubilization solution was added to each well. The absorbance at 450 nm was read the following day. Half-Maximal inhibitory concentrations (IC_{50}) were determined using Sigma Plot 9.0 software (Systat Software Inc.).

4.1.4. Western blot analysis

Pancreatic cancer cells Capan-1 with higher expressing P-STAT3 were seeded in 10 cm plates. The next day, cells were treated or untreated with XZH-5 (25, 50, 75 μM) or **1d** (15, 25 μM) at 60–70% confluence. After 24 h, the cells were harvested and analyzed by western blot. The results are shown in Supporting information Figure S1.

4.2. Chemical methods

All reagents were obtained from Sigma–Aldrich, Acros Organics and appTec and were of analytical grade. No further purification was performed unless specified. Solvents were obtained from commercial sources and dried utilizing standard procedures. ^{1}H and ^{13}C spectra were obtained from Bruker 200 MHz, 300 MHz and 500 MHz instrument systems. The chemical shifts are reported in parts per million (δ, ppm): in $CDCl_3$ (^{1}H NMR: δ = 7.24 ppm, ^{13}C: 77.0 ppm) and in DMSO-d_6 (^{1}H NMR: δ = 2.49 ppm, ^{13}C: 39.5 ppm). The coupling constants are in hertz (Hz) and multiplicity is reported as s (singlet), d (doublet), t (triplet), m (multiplet) and br (broad). Mass spectra were collected on Bruker ESQUIRE-LCMS. The reaction progress was monitored by TLC on silica coated plates. Flash chromatography was performed using silica gel.

4.2.1. General procedure for the synthesis of 1a, 1b, 1i, and 1h

N-Methyl methyl histidine hydrochloride (1.0 equiv), *N*-Boc amino acid (1.2 equiv), DCC (1.2 equiv), HOBt (1.2 equiv) and TEA (2.0 equiv) were charged in a flask and stirred at room temperature for 3 days by which time TLC showed no starting materials. The reaction mixture was filtrated and the filtrate was washed with aqueous $NaHCO_3$ (three times) and then with water (one time). The organic phase was dried over magnesium sulfate and the filtrate was evaporated under reduced pressure and purified using column chromatography (silica gel, eluent DCM/methanol) to afford solid products. The product was then treated with DCM/TFA (3/1 v/v) and the resulting mixture was stirred overnight to give an oily yellowish product after the removal of the solvent. This Boc deprotected product (1.0 equiv) was treated with 1.2 equiv of 1-isocyanato-3,5-bis(trifluoromethyl) benzene in the presence of TEA (5.0 equiv) in DCM. The reaction mixture was stirred at room temperature overnight until TLC showed no starting material. The mixture was then washed with aqueous $NaHCO_3$ and water. The organic layer was concentrated under reduced pressure. The resulting yellowish solid was purified using column chromatography (silica gel, eluent DCM/methanol) to give white solid product.

4.2.1.1. Methyl-2-((*S*)-2-(3-(3,5-bis(trifluoromethyl)phenyl)ureido)-3-methylbutanamido)-3-(1-methyl-1*H*-imidazol-4-yl)propanoate (1a). White solid. Mp, 165 °C. ^{1}H NMR (500 MHz, $CDCl_3$) δ 0.83–0.91 (m, 6H), 1.98–2.50 (m, 1H), 2.80 (m, 1H), 3.50 (s, 3H), 3.58(s, 3H), 4.15–4.18 (m, 1H), 4.47–4.52 (m, 1H), 6.54 (d, *J* = 8.5 Hz, 1H), 6.86 (s, 1H), 7.42 (s, 1H), 7.56 (s, 1H), 8.00 (s, 2H), 8.51 (d, *J* = 7 Hz, 1H), 9.41(s, 1H). ^{13}C NMR (125 Hz, $CDCl_3$) δ 18.0, 19.2, 29.0, 31.6, 33.2, 52.2, 53.2, 59.1, 114.8, 118.0, 118.1, 122.2, 124.4,131.5, 131.8, 137.0, 137.6, 141.3, 155.2, 171.4, 173.7. MS (ESI) 538.1 $(M+H)^+$.

4.2.1.2. Methyl-2-((*S*)-2-(3-(3,5-bis(trifluoromethyl)phenyl)propanamido-3-3(1-methyl-1*H*-imidazol-4-yl)propanoate (1b). White solid. Mp, 208 °C. ^{1}H NMR (500 MHz, $CDCl_3$) δ 1.24 (d, *J* = 6.6 Hz, 3H), 2.76–2.590 (m, 2H), 3.53–3.60 (m, 6H), 4.24–4.28 (m, 1H), 4.46–4.48 (m, 1H), 6.67 (d, *J* = 7.2 Hz, 1H), 6.85 (s, 1H), 7.41 (s, 1H), 7.55 (s, 1H), 8.01 (s, 2H), 8.48 (d, *J* = 7.5 Hz, 1H), 9.40 (s, 1H). ^{13}C NMR (125 Hz, $CDCl_3$) δ 19.6, 30.2, 33.0, 33.3, 52.5, 52.8, 117.5, 118.3, 118.4, 122.7, 124.9, 130.8, 131.0, 131.3, 137.3, 142.8, 154.5, 172.4, 173.0. MS (ESI) 510.2 $(M+H)^+$.

4.2.1.3. Methyl-2-(2-(3-(3,5-bis(trifluoromethyl)phenyl)ureido)-3-(2*H*-isoindol-1-yl)propanamido)-3-(1-methyl-1*H*-imidazol-4-yl)propanoate (1h). White solid. Mp, 201 °C. ^{1}H NMR (500 MHz, $CDCl_3$) δ 2.86–2.99 (m, 2H), 3.00–3.03 (m, 1H), 3.17–3.22 (m, 1H), 3.53 (s, 3H), 3.63 (s, 3H), 4.53–4.57 (m, 2H), 6.49–6.50 (m, 1H), 6.85 (s, 1H), 6.94–6.97 (m, 1H), 7.04–7.07 (m, 1H), 7.14 (s, 1H), 7.32–7.42 (m, 1H), 7.55–7.60 (m, 2H), 7.98 (s, 2H), 8.64 (s, 1H), 9.41 (s, 1H), 10.87 (s, 1H). ^{13}C NMR (125 Hz, $CDCl_3$) δ 28.6, 30.4, 32.1, 33.1, 52.6, 52.9, 53.8, 109.8, 117.5, 118.2, 118.4, 118.9, 119.0, 122.7, 124.9, 127.1,128.0, 131.1, 131.3, 136.6, 137.3, 142.8, 154.7, 172.2, 172.5. MS (ESI) 625.2 $(M+H)^+$.

4.2.1.4. (3*S*)-Benzyl 3-(3-(3,5-bis(trifluoromethyl)phenyl)ureido)-4-((1-methoxy-3-(1-methyl-1*H*-imidazol-4-yl)-1-oxopropan-2-yl)amino)-4-oxobutanoate (1i). White solid: ^{1}H NMR (500 MHz, $CDCl_3$) δ 2.87–2.92 (m, 1H), 3.02–3.07 (m, 3H), 3.49 (s, 3H), 3.57 (s, 3H), 4.72–4.76 (m, 1H), 4.87–4.90 (m, 1H), 5.02–5.08 (q, 2H), 6.66 (s, 1H), 6.80 (d, *J* = 8.5 Hz, 1H), 7.24 (s, 6H), 7.35 (s, 1H), 7.82 (s, 2H), 8.06 (d, *J* = 7.5 Hz, 1H), 9.00 (s, 1H). ^{13}C NMR (125 Hz, $CDCl_3$) δ 29.2, 33.4, 36.6, 50.0, 52.4, 52.7, 66.8, 115.1, 118.0, 118.4, 122.2, 124.4, 128.1, 128.5, 135.4, 136.6, 137.5, 141.3, 154.7, 171.3, 173.4, 171.9. MS (ESI) 644.2 $(M+H)^+$.

4.2.2. General synthesis of 1d, 1c, 1g, 1k, 1l, 1j, 1n, and 1m

N-Methyl methyl histidine hydrochloride (1 equiv), Boc amino acid (1.2 equiv), BOP (1.2 equiv) and TEA (2.0 equiv) were charged in flask and the resulting reaction was stirred at room temperature for 3 days by which time TLC showed no starting material. The reaction mixture was washed with aqueous $NaHCO_3$ (three times) and with water (one time). The organic phase was dried over

magnesium sulfate and was then evaporated under reduced pressure. The resulting residue was purified using column chromatography (silica gel, eluent DCM/methanol) to give a solid product. The product was then treated with DCM/TFA (3:1) and stirred overnight to afford an oily yellowish product. This Boc deprotected product (1.0 equiv) was treated with 1.2 equiv of 1-isocyanato-3,5-bis(trifluoromethyl)benzene in the presence of TEA (5.0 equiv) in DCM. The reaction mixture was stirred at room temperature overnight until TLC showed no starting material. The mixture was then washed with aqueous $NaHCO_3$ and water. The organic layer was evaporated under reduced pressure. The yellowish solid residue was purified using column chromatography (silica gel, eluent DCM/methanol) to yield a white solid.

4.2.2.1. Methyl-2-((*S*)-2-(3-(3,5-bis(trifluoromethyl)phenyl)ureido)-4-methylpentanamido)-3-(1-methyl-1*H*-imidazol-4-yl)propanoate (1c). White solid. Mp, 180 °C. ^{1}H NMR (500 MHz, $CDCl_3$) δ 0.94–0.96 (m, 6H), 1.51–1.58 (m, 1H), 1.62–165 (m, 1H),1.67–1.81 (m, 1H), 3.12–3.13 (m, 2H), 3.58 (s, 3H), 3.67 (s, 3H), 4.40–4.44 (m, 1H), 4.72–4.75(m, 1H), 6.69–6.71 (m, 1H), 6.76 (m, 1H), 7.28 (S, 1H), 7.37 (s, 1H), 7.73 (m, 2H), 8.21–8.23 (m, 1H), 8.44 (s, 1H). ^{13}C NMR (125 Hz, $CDCl_3$) δ 21.9, 22.8, 24.7, 28.9, 33.3, 41.9, 52.3, 52.6, 52.9, 117.7, 118.3, 122.2, 124.4, 131.2, 131.5, 131.7, 132.0, 136.7, 137.5, 141.2, 154.9, 171.4, 175.1. MS (ESI) 552.2 $(M+H)^+$.

4.2.2.2. (*R*) Methyl-2-((2*S*,3*R*)-2-(3-(3,5-bis(trifluoromethyl)phenyl)ureido)-3-methylpentanamido)-3-(1-methyl-1*H*-imidazol-4-yl)propanoate (1d). White solid. Mp, 183 °C. ^{1}H NMR (500 MHz, $CDCl_3$) δ 1.0–1.01 (m, 6H), 1.02–1.25 (m, 1H), 1.55–1.60 (m, 1H), 1.81–1.84 (m, 1H), 3.07–3.08 (m, 2H), 3.56 (s, 3H), 3.64 (s, 3H), 4.35–4.38 (m, 1H), 4.69–4.72(m, 1H), 6.68 (s, 1H), 6.75–6.78 (m, 1H), 7.31–7.33 (m, 2H), 7.80 (s, 2H), 8.29–8.30 (m, 1H), 8.44 (s, 1H). ^{13}C NMR (125 Hz, $CDCl_3$) δ 11.2, 15.4,25.0, 28.9, 33.3, 37.9, 52.3, 53.2, 58.5, 114.9, 118.0, 118.2, 122.2, 124.4, 131.3, 131.8, 131.6, 131.8, 132.1, 136.8, 137.6, 141.3, 155.1, 171.2, 173.7. MS (ESI) 552.2 $(M+H)^+$.

4.2.2.3. Methyl-2-((*S*)-2-(3-(3,5-bis(trifluoromethyl)phenyl)ureido)-3-phenylpropanamido)-3-(1-methyl-1*H*-imidazol-4-yl)propanoate (1g). White solid. Mp, 92 °C. ^{1}H NMR (500 MHz, $CDCl_3$) δ 2.92–2.99 (m, 1H), 3.06–3.14 (m, 3H), 3.56 (s, 3H), 3.66 (s, 3H), 4.69–4.74 (m, 2H), 6.59–6.69 (m, 2H), 7.13–7.26 (m, 7H), 7.34 (s, 1H), 7.82 (s, 2H), 8.00 (s, 1H), 8.48 (s, 1H). ^{13}C NMR (125 Hz, $CDCl_3$) δ 29.1, 33.3, 38.7, 52.4, 53.0, 55.2, 115.0, 117.9, 118.3, 126.9, 128.4, 128.5, 129.3, 129.5, 131.6, 131.9, 137.5, 141.1, 154.8, 171.3, 173.1. MS (ESI) 586.2 $(M+H)^+$.

4.2.2.4. (4*S*)-Benzyl-4-(3-(3,5-bis(trifluoromethyl)phenyl)ureido)-5-((1-methoxy-3-(1-methyl-1*H*-imidazol-4-yl)-1-oxopropan-2-yl)-amino)-5-oxopentanoate (1j). White solid: ^{1}H NMR (500 MHz, $CDCl_3$) δ 1.97–2.02(m, 2H), 2.17–2.18 (m, 1H), 2.51–2.54 (m, 2H), 3.08–3.09 (m, 2H), 3.53 (s, 3H), 3.61 (s, 3H), 4.52–4.54 (m, 1H), 4.50–4.75 (m, 1H), 5.07 (s, 2H), 6.71 (s, 2H), 7.24–7.37 (m, 7H), 7.81 (s, 2H), 8.13–8.14 (m, 1H), 8.55 (m, 1H). ^{13}C NMR (125 Hz, $CDCl_3$) δ 28.0, 28.8, 30.3, 33.6, 52.5, 52.8, 53.1, 66.5, 118.0, 118.6, 122.2, 124.4, 128.1, 128.2, 128.5, 131.6, 131.9, 135.8, 136.0, 137.3, 141.2, 154.9, 171.2, 173.0, 173.2. MS (ESI) 658.3 $(M+H)^+$.

4.2.2.5. Methyl-2-((*S*)-2-(3-(3,5-bis(trifluoromethyl)phenyl)ureido)-3-methylbutanamido)-3-(1-ethyl-1*H*-imidazol-4-yl)propanoate (1k). White solid. Mp, 164 °C. ^{1}H NMR (500 MHz, $CDCl_3$) δ 0.94–1.03 (m, 6H), 1.35–1.38 (t, 3H), 2.07–2.11 (m, 1H), 3.06–3.08 (m, 2H), 3.62 (s, 3H), 3.84–3.89 (q, 2H), 4.35–4.38 (m, 1H), 4.68–4.70 (m, 1H), 6.73–6.78 (m, 2H), 7.31 (s, 1H), 7.37 (s, 1H), 7.79 (s, 2H), 8.37–8.39 (m, 1H), 8.50 (s, 1H). ^{13}C NMR (125 Hz, $CDCl_3$) δ 16.0, 18.1, 19.3, 29.0, 31.7, 41.9, 52.2, 53.3, 59.3, 116.4, 118.0, 122.2, 124.4, 131.3, 131.6, 131.8, 132.1, 136.4, 136.9, 141.3, 155.2, 171.3, 173.7. MS (ESI) 552.2 $(M+H)^+$.

4.2.2.6. Methyl-2-((*S*)-2-(3-(3,5-bis(trifluoromethyl)phenyl)ureido)-3,3-dimethylbutanamido)-3-(1-methyl-1*H*-imidazol-4-yl)propanoate (1l). White solid: ^{1}H NMR (500 MHz, $CDCl_3$) δ 1.07 (s, 9H), 2.99–3.09 (m, 2H), 3.58 (s, 3H), 3.65 (s, 3H), 4.35–4.37 (m, 1H), 4.62–4.65 (m, 1H), 6.66 (m, 1H), 6.72–6.74 (m, 1H), 7.33–7.35 (m, 2H), 7.81(s, 2H), 8.27–8.29 (m, 1H), 8.44 (s, 1H). ^{13}C NMR (125 Hz, $CDCl_3$) δ 26.7, 29.0, 33.3, 34.7, 52.1, 53.1, 61.6, 118.1, 122.2, 124.4, 131.5, 131.8, 136.9, 137.5, 141.4, 155.3, 171.5, 172.1. MS (ESI) 552.2 $(M+H)^+$.

4.2.2.7. Methyl-3-(1-methyl-1*H*-imidazol-4-yl)-2-((*S*)-3-methyl-2-(3-(3-(trifluoromethyl)phenyl)ureido)butanamido)propanoate (1m). White solid: ^{1}H NMR (500 MHz, $CDCl_3$) δ 0.98–1.05 (m, 6H), 2.10–2.14 (m, 1H), 3.07–3.08 (m, 2H), 3.53 (s, 3H), 3.66 (s, 3H), 4.39–4.42 (m, 1H), 4.75–4.79 (m, 1H), 6.69 (m, 1H), 6.78–6.80 (m, 1H), 7.12–7.14 (m, 1H), 7.20–7.23(m, 1H), 7.29 (s, 1H), 7.34–7.36 (m, 1H), 7.73 (s, 1H), 8.27–8.29 (m, 1H), 8.34 (s, 1H). ^{13}C NMR (125 Hz, $CDCl_3$) δ 18.1, 19.2, 29.2, 31.7, 33.2, 52.2, 53.0, 59.1, 115.4, 118.1, 118.5, 121.8 123.0, 129.1, 130.7, 131.0, 137.0, 137.6, 140.2, 155.6, 171.5, 173.5. MS (ESI) 470.2 $(M+H)^+$.

4.2.2.8. Methyl-2-((*S*)-2-(3-(3,5-bis(trifluoromethyl)phenyl)ureido)-3-methylbutanamido)-3-(1*H*-imidazol-4-yl)propanoate (1n). White solid. Mp, 158 °C. ^{1}H NMR (500 MHz, $CDCl_3$) δ 0.81–0.89 (m, 6H), 1.97–2.02 (m, 1H), 2.86–2.94 (m, 2H), 3.57 (s, 3H), 4.17–4.20 (m, 1H), 4.48–4.53(m, 1H), 6.54 (d, J = 8.5 Hz, 1H), 6.81 (s, 1H), 7.50 (s, 1H), 7.56 (s, 1H), 7.99 (s, 2H), 8.52 (d, J = 7 Hz, 1H), 9.42 (s, 1H), 11.80 (s, 1H). ^{13}C NMR (125 Hz, $CDCl_3$) δ 17.5, 19.0,36.5, 336.6, 52.2, 52.4, 59.1, 114.4, 117.7, 117.9, 122.2, 124.3, 131.5, 131.8, 134.4, 141.5, 155.4, 170.9, 172.3. MS (ESI) 524.2 $(M+H)^+$.

4.2.3. General synthesis of 1e and 1f

1.0 equiv of **1a** or **1b** was dissolved in THF/MeOH/water (v, 3:1:1). The solution was chilled to 0 °C after which 1.5 equiv of $LiOH{\cdot}H_2O$ was added, and the resulting mixture was stirred at room temperature for about 2 h until TLC showed no starting material. After which THF and MeOH were removed under reduced pressure and the aqueous phase was neutralized using 10% HCl (aqueous) to pH 4–5. The mixture was then extracted with a 1:1 (v) mixture of chloroform/isopropanol. The organic extract was then dried over magnesium sulfate and the solvent removed to give a white solid.

4.2.3.1. 2-((*S*)-2-(3-(3,5-Bis(trifluoromethyl)phenyl)ureido)-3-methylbutanamido)-3-(1-methyl-1*H*-imidazol-4-yl)propanoic acid (1e). White soild. ^{1}H NMR (500 MHz, $CDCl_3$) δ 0.73–0.76 (m, 6H), 2.03–2.05 (m, 1H), 2.73–3.22 (m, 2H), 3.45–3.69 (m, 3H), 4.10–4.35 (m, 3H), 6.91 (s, 1H), 7.22–7.44(m, 1H), 7.51–7.77 (d, 3H), 10.40 (s, 1H). MS (ESI) 522.0 $(M-H)^-$.

4.2.3.2. 2-((*S*)-2-(3-(3,5-Bis(trifluoromethyl)phenyl)ureido) propanamido)-3-(1-methyl-1*H*-imidazol-4-yl)propanoic acid (1f). White solid. ^{1}H NMR (500 MHz, $CDCl_3$) δ 1.26 (d, J = 7 Hz, 3H), 2.88–3.07 (m, 2H), 3.55 (s, 3H), 3.75–3.80 (m, 1H), 4.24–4.27 (t, 1H), 4.49–4.50 (m, 1H), 6.81 (d, J = 7 Hz 1H), 7.17 (s, 1H), 7.56 (s, 1H) 8.05 (s, 2H), 8.20 (s, 1H), 8.45 (d, J = 8 Hz, 1H), 9.76 (s, 1H).

Acknowledgments

R.C.P. and H.W. were supported by institutional funds from Miami University. J.L. acknowledges AACR-Pancreatic Cancer Action Network Innovation grant.

Supplementary data

Supplementary data associated with this article can be found, in the online version, at http://dx.doi.org/10.1016/j.bmc.2015.01.025.

References and notes

1. Hirano, T.; Ishihara, K.; Hibi, N. *Oncogene* **2000**, *19*, 2548.
2. Bromberg, J.; Darnell, J. E., Jr. *Oncogene* **2000**, *19*, 2468.
3. Darnell, J. E., Jr. *Science* **1997**, *277*, 1630.
4. Darnell, J. E.; Kerr, I. M.; Stark, G. R. *Science* **1994**, *264*, 1415.
5. Darnell, J. E. *Science* **1997**, *277*, 1630.
6. Turkson, J.; Jove, R. *Oncogene* **2000**, *19*, 6613.
7. Levy, D. E.; Darnell, J. E. *Nat. Rev. Mol. Cell Biol.* **2002**, *3*, 651.
8. Bowman, T.; Garcia, R.; Turkson, J.; Jove, R. *Oncogene* **2000**, *19*, 2474.
9. Yu, H.; Jove, R. *Nat. Rev. Cancer* **2004**, *4*, 97.
10. Darnell, J. E., Jr. *Nat. Rev. Cancer* **2002**, *2*, 740.
11. Kraskouskay, D.; Duodu, E.; Arpinw, C. C.; Gunning, P. T. *Chem. Soc. Rev.* **2013**, *42*, 3337.
12. Costantino, L.; Barlocco, D. *Curr. Med. Chem.* **2008**, *15*, 834.
13. Lavecchia, A.; Di Giovanni, C.; Novellino, E. *Curr. Med. Chem.* **2011**, *18*, 2359.
14. Redell, M. S.; Tweardy, D. J. *Curr. Pharm. Des.* **2005**, *11*, 2873.
15. Catlett-Falcone, R.; Landowski, T. H.; Oshiro, M. M.; Turkson, J.; Levitzki, A.; Savino, R.; Ciliberto, G.; Moscinski, L.; Fernandez-Luna, J. L.; Nunez, G.; Dalton, W. S.; Jove, R. *Immunity* **1999**, *10*, 105.
16. Ling, X.; Arlinghaus, R. B. *Cancer Res.* **2005**, *65*, 2532.
17. Gao, L.; Zhang, L.; Hu, J.; Li, F.; Shao, Y.; Zhao, D.; Kalvakolanu, D. V.; Kopecko, D. J.; Zhao, X.; Xu, D. Q. *Clin. Cancer Res.* **2005**, *11*, 6333.
18. Barton, B. E.; Murphy, T. F.; Shu, P.; Huang, H. F.; Meyenhofer, M.; Barton, A. *Mol. Cancer Ther.* **2004**, *3*, 1183.
19. Leong, P. L.; Andrews, G. A.; Johnson, D. E.; Dyer, K. F.; Xi, S.; Mai, J. C.; Robbins, P. D.; Gadiparthi, S.; Burke, N. A.; Watkins, S. F.; Grandis, J. R. *Proc. Natl. Acad. Sci. U.S.A.* **2003**, *100*, 4138.
20. Pedranzini, L.; Dechow, T.; Berishaj, M.; Comenzo, R.; Zhou, P.; Azare, J.; Bornmann, W.; Bromberg, J. *Cancer Res.* **2006**, *66*, 9714.
21. Nam, S.; Buettner, R.; Turkson, J.; Kim, D.; Cheng, J. Q.; Muehlbeyer, S.; Hippe, F.; Vatter, S.; Merz, K.-H.; Eisenbrand, G.; Jove, R. *Proc. Natl. Acad. Sci. U.S.A.* **2005**, *102*, 5998.
22. Kotha, A.; Sekharam, M.; Cilenti, L.; Siddiquee, K.; Khaled, A.; Zervos, A. S.; Carter, B.; Turkson, J.; Jove, R. *Mol. Cancer Ther.* **2006**, *5*, 621.
23. Blaskovich, M. A.; Sun, J.; Cantor, A.; Turkson, J.; Jove, R.; Sebti, S. M. *Cancer Res.* **2003**, *63*, 1270.
24. Sun, J.; Blaskovich, M. A.; Jove, R.; Livingston, S. K.; Coppola, D.; Sebti, S. M. *Oncogene* **2005**, *24*, 3236.
25. Shimizu, M.; Weinstein, I. B. *Mutat. Res.* **2005**, *591*, 147.
26. Ren, Z.; Cabell, L. A.; Schaefer, T. S.; McMurray, J. S. *Bioorg. Med. Chem. Lett.* **2003**, *13*, 633.
27. Chen, J.; Nikolovska-Coleska, Z.; Yang, C.-Y.; Gomez, C.; Gao, W.; Krajewski, K.; Jiang, S.; Roller, P.; Wang, S. *Bioorg. Med. Chem. Lett.* **2007**, *17*, 3939.
28. Coleman, D. R.; Ren, Z.; Mandal, P. K.; Cameron, A. G.; Dyer, G. A.; Muranjan, S.; Campbell, M.; Chen, X.; McMurray, J. S. *J. Med. Chem.* **2005**, *48*, 6661.
29. Siddiquee, K. A.; Gunning, P. T.; Glenn, M.; Katt, W. P.; Zhang, S.; Schroeck, C.; Sebti, S. M.; Jove, R.; Hamilton, A. D.; Turkson *ACS Chem. Biol.* **2007**, *2*, 787.
30. Zhang, X.; Yue, P.; Fletcher, S.; Zhao, W.; Gunning, P. T.; Turkson, J. *Biochem. Pharmacol.* **2010**, *79*, 1398.
31. Mandal, P. K.; Liao, W. S.-L.; McMurray, J. S. *Org. Lett.* **2009**, *11*, 3394.
32. Chen, J.; Bai, L.; Bernard, D.; Nikolovska-Coleska, Z.; Gomez, C.; Zhang, J.; Yi, H.; Wang, S. *ACS Med. Chem Lett.* **2010**, *1*, 85.
33. Gomez, C.; Bai, L.; Zhang, J.; Nikolovska-Coleska, Z.; Chen, J.; Yi, H.; Wang, S. *Bioorg. Med. Chem. Lett.* **2009**, *19*, 1733.
34. Ren, X.; Duan, L.; He, Q.; Zhang, Z.; Zhou, Y.; Wu, D.; Pan, J.; Pei, D.; Ding, K. *ACS Med. Chem. Lett.* **2010**, *1*, 454.
35. Yu, Z.-Y.; Huang, R.; Xiao, H.; Sun, W.-F.; Shan, Y.-J.; Wang, B.; Zhao, T.-T.; Dong, B.; Zhao, Z.-H.; Liu, X.-L.; Wang, S.-Q.; Yang, R.-F.; Luo, Q.-L.; Cong, Y.-W. *Int. J. Cancer* **2010**, *127*, 1259.
36. Liu, A.; Liu, Y.; Xu, Z.; Yu, W.; Wang, H.; Li, C.; Lin, J. *Cancer Sci.* **2011**, *102*, 1381.
37. Liu, Y.; Liu, A.; Xu, Z.; Yu, W.; Wang, H.; Li, C.; Lin, J. *Apoptosis* **2011**, *16*, 502.
38. Liu, A.; Liu, Y.; Jin, Z.; Hu, Q.; Lin, L.; Jou, D.; Yang, J.; Xu, Z.; Wang, H.; Li, C.; Lin, J. *PLoS ONE* **2012**, *7*, e46624.
39. Jain, R.; Cohen, L. A. *Tetrahedron* **1996**, *52*, 5363.
40. Purser, S.; Moore, P. R.; Swallowb, S.; Gouverneur, V. *Chem. Soc. Rev.* **2008**, *37*, 320.
41. Davis, I. W.; Raha, K.; Head, M. S.; Baker, D. *Protein Sci.* **1998**, *2009*, 18.
42. Davis, I. W.; Baker, D. *J. Mol. Biol.* **2009**, *385*, 381.
43. Meiler, J.; Baker, D. *Proteins: Struct., Funct., Bioinf.* **2006**, *65*, 538.
44. Cheng, T.; Zhao, Y.; Li, X.; Lin, F.; Xu, Y.; Zhang, X. *J. Chem. Inf. Model* **2007**, *47*, 2140.
45. Roy, A.; Kucukural, A.; Zhang, Y. *Nat. Protoc.* **2010**, *5*, 725.
46. Becker, S.; Groner, B.; Müller, C. W. *Nature* **1998**, *394*, 145.
47. Chaudhury, S.; Berrondo, M.; Weitzner, B. D.; Muthu, P.; Bergman, H.; Gray, J. J. *PLoS ONE* **2011**, *6*, e22477.
48. Moriarty, N. W.; Grosse-Kunstleve, R. W.; Adams, P. D. *Acta Crystallogr., Sect. D Biol. Crystallogr.* **2009**, *65*, 1074.
49. Hawkins, P. C. D.; Skillman, A. G.; Warren, G. L.; Ellingson, B. A.; Stahl, M. T. *J. Chem. Inf. Model.* **2010**, *50*, 572.